GEOMAGNETIC ANOMALIES OVER THE MORAINE FIELD TO THE NORTH OF MIZUHO STATION, EAST ANTARCTICA

Kazuo SHIBUYA

National Institute of Polar Research, 9–10, Kaga 1-chome, Itabashi-ku, Tokyo 173

Abstract: By using the total intensity data of two aeromagnetic survey flights by the 21st Japanese Antarctic Research Expedition, geomagnetic anomalies over the moraine field to the north of Mizuho Station are obtained. The reduced geomagnetic anomaly profile for each survey flight has a relative uncertainty of 20–30 nT, and the hand contouring is made at intervals of 100 nT. The obtained geomagnetic anomalies have a short wave-length (10–30 km) variation from −200 nT to 200–300 nT with the associated anomaly eyes of 400–500 nT amplitude. The free-air gravity anomalies in Mizuho Plateau suggest the existence of a subglacial mound of about 2400 m bedrock height, and the aeromagnetically surveyed area is situated at the periphery of such subglacial mound. The obtained short wave-length geomagnetic anomalies may be related to the steep change of bedrock geology beneath the 2000 m thick ice sheet.

1. Introduction

An aeromagnetic survey plays an important role in the study of geological structure of Antarctica where 97% of the area is covered with the thick ice sheet. It is also useful for the interpretation of bedrock topography beneath the ice mass as exampled for the Shirase Glacier region by SHIBUYA and TANAKA (1983). In this report, the analysis is made for the survey flights along the traverse route from Syowa to Mizuho Stations and over the moraine field north of Mizuho Station (Fig. 1), and the geomagnetic anomalies are obtained. Since the outline of the flight method, observation system and diurnal information is reported in detail in SHIBUYA (1984), the necessary data in this analysis are briefly summarized in the second section. As the positioning has some uncertainty, its effect on the obtained anomaly is discussed. The obtained geomagnetic anomaly contours are superposed on the previously obtained free-air gravity anomaly contours of the same area, and the geophysical structure of the area concerned is discussed.

2. Survey and Data

The survey flights were made by the 21st Japanese Antarctic Research Expedition (JARE-21) on November 3, 1980 and on January 2, 1981. Figure 1 shows the courses of Flight M1, Flight M2 and Flight M4. Here Flight M2 gives a reverse profile of Flight M1 along the traverse route from Syowa to Mizuho Stations (Routes S–H–Z). Flight M4 is along the Mizuho Station–S122 portion of Routes S–H–Z and then covers the moraine field which was found by JARE-10 and surveyed by the

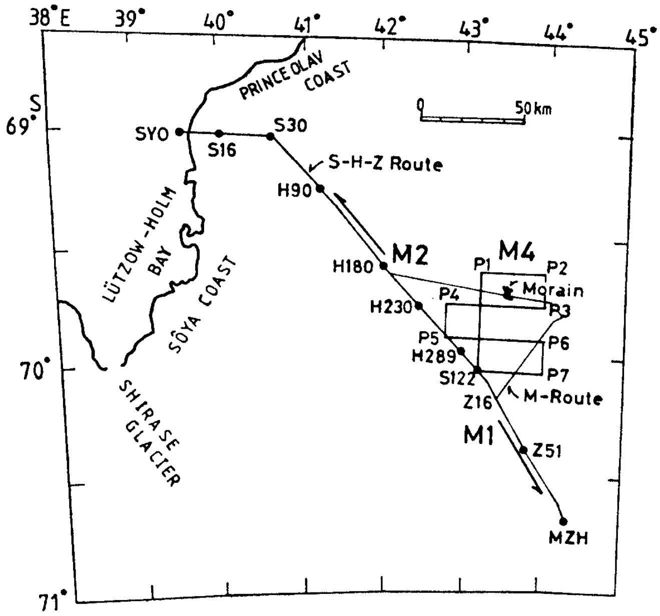

Fig. 1. Routes S–H–Z and Route M. Flight M1 is 300–500 m shifted to the downstream direction of the ice sheet against the traverse route and Flight M2 is 300–500 m shifted to the upstream direction. Flight M4 covers a part of the moraine field making a mosaic flight course. S16, S30 etc. indicate marker station names. P1 to P7 are postulated turning points on the flight course. SYO and MZH are abbreviations of Syowa and Mizuho Stations.

oversnow traverse party of JARE-14 (SHIMIZU, 1978). The moraine field on Route M (see Fig. 1) is so named because thin ice-covered rocky area was found in the blue ice region where no bedrocks occur nearby. The moraine field is considered to be situated on the western slope of the ice mound which was revealed by the traverse survey (NARUSE and YOKOYAMA, 1975).

Table 1 summarizes the log of each flight. The flight height was controlled at 457 m (1500 ft) above the ice sheet surface by the radar altimeter and the height above sea level was monitored by the barometer. The flight speed was controlled at an instrumental speed of 100 knots by the speed-meter of Pilatus Porter PC-6. The positioning by a VLF/omega receiver (upper row in each remark column) sometimes gave erroneous data up to an offset of 1.5–7.5 km for the known position (lower row in each remark column which is re-tabulated from NARUSE and YOKOYAMA, 1975). Then the analyses are proceeded on the basis of the passing time of each marker station for Flight M1 and Flight M2, because the associated uncertainty of ±300 m for each marker positioning is quite smaller than the above offset value.

The "spur" of the oversnow vehicles along Routes S–H–Z was effective in keeping the flight course on the route. Considering the calculated interval velocity and the number of measured total intensity data points between the neighboring marker stations, the coordinate values (latitude, longitude, height) are assigned to each data point by the method of proportional distribution. Because of the uncertainties of

Table 1. Logs of Flight M1, Flight M2 and Flight M4. For details of positioning, see text.

Flight M1 (0930–1100 LT, November 3, 1980)

Control point	Departure time	Distance (km)	Estimate time of flight	Estimate time of arrival	Actual time of arrival	Magnetic course (degree)	Sampling distance (m)	Remark
S 16	$09^{h}39^{m}00^{s}$							69°01′54″S 40°02′30″E 69 01 55 40 02 56
		25.9	$8^{m}30^{s}$	$09^{h}47^{m}30^{s}$	$09^{h}47^{m}30^{s}$	145	61.3	
S 30	09 47 30							69°01′18″S 40°40′00″E 69 03 01 40 42 13
		31.5	10 00	09 57 30	09 57 00	179	67.3	
H90	09 57 00							69°15′30″S 41°15′00″E 69 15 44 41 15 09
		48.2	16 00	10 13 00	10 11 00	182	66.7	
H180	10 11 00							69°31′00″S 41°59′00″E 69 35 18 42 00 36
		29.6	9 30	10 20 30	10 19 00	186	66.0	
H230	10 19 00							69°47′00″S 42°23′00″E 69 46 12 42 27 06
		29.6	9 30	10 28 30	10 28 30	185	64.8	
H289	10 28 30							69°59′02″S 42°58′01″E
		7.4	2 30	10 31 00	10 31 00	186	66.1	
S 122	10 31 00							70°01′06″S 43°06′30″E 70 01 15 43 09 24
		44.4	14 30	10 45 30	—	195	64.4	
Z51	10 46 00	change course						unidentified 70°22′12″ 43°47′00″
		42.6	14 00	11 00 00	10 58 00	195	64.4	
Mizuho Station	10 58 00	(arrival)						70°42′06″S 44°17′30″E 70 41 53 44 19 54

Table 1 (continued).

Flight M2 (1320–1530 LT, November 3, 1980)

Control point	Departure time	Distance (km)	Estimate time of flight	Estimate time of arrival	Actual time of arrival	Magnetic course (degree)	Sampling distance (m)	Remark
Mizuho Station	$13^{h}37^{m}00^{s}$							
		42.6	$14^{m}00^{s}$	$13^{h}51^{m}00^{s}$	——	016	63.8	
Z51	13 51 00	change course						unidentified
		44.4	14 30	14 05 30	$14^{h}04^{m}30^{s}$	015	63.8	
S122	14 04 30							
		7.4	3 00	14 07 30	——	337	62.5	
H289	14 07 30	change course						unidentified
		29.6	9 30	14 17 00	14 17 00	006	62.5	
H230	14 17 00							
		29.6	9 30	14 26 30	14 25 30	005	62.0	
H180	14 25 30							
		48.2	15 30	14 41 00	14 40 00	006	64.4	
H90	14 40 00							
		31.5	10 00	14 50 00	14 48 50	002	63.9	
S30	14 56 00							circular flight 7 min
		25.9	8 30	15 04 30	15 02 00	320	65.1	
S16	15 02 00							
		18.5	6 00	15 08 00	15 08 00	325	61.5	
Syowa Station	15 08 00	(arrival)						

Table 1 (continued).

Flight M4 (1300–1600 LT, January 2, 1981)

Start Mizuho Station	at $13^{h}05^{m}40^{s}$			
Depart S122	at $13^{h}31^{m}10^{s}$	and flew 15 min	to north with 45°	magnetic course
Through P1	at $13^{h}46^{m}10^{s}$	and flew 10 〃	to east with 135°	〃
Through P2	at $13^{h}56^{m}10^{s}$	and flew 5 〃	to south with 225°	〃
Through P3	at $14^{h}01^{m}10^{s}$	and flew 15 〃	to west with 315°	〃
Through P4	at $14^{h}16^{m}10^{s}$	and flew 5 〃	to south with 225°	〃
Through P5	at $14^{h}21^{m}10^{s}$	and flew 15 〃	to east with 135°	〃
Through P6	at $14^{h}36^{m}10^{s}$	and flew 5 〃	to south with 225°	〃
Through P7	at $14^{h}41^{m}10^{s}$	and flew 10 〃	to west with 315°	〃

the passing time of each marker station, etc., the spatial sampling density of total intensity data (8th column in Table 1) is not uniform and ranges 61.3–67.3 m/point for Flight M1 and 61.5–65.1 m/point for Flight M2, respectively. The spatial sampling density thus fluctuates 8% against the presumed rate of 62 m/point for the constant speed of 100 knots and 1.2-s sampling rate of total intensity data and is considered to have time variation. The analyses are proceeded, however, assuming the uniform interval velocity of the aircraft in each segment of the flight profile.

As for Flight M4, the course started from Mizuho Station and was along Routes S–H–Z and departed at S122 to pass through the postulated turning point P1, P2, etc., returning to S122 making a mosaic figure as illustrated in Fig. 1. There were no markers or outcrops for reliable positioning except the starting points Mizuho Station and S122. As listed in Table 1, the mosaic flight was based on the flight time with keeping the magnetic course and the instrumental speed as constant as possible. Because of the wind, the mosaic course did not close actually and the effect of wind speed and wind direction has to be considered in the data reduction procedure.

3. Reduction to Geomagnetic Anomaly

Since the method of reduction from the observed total intensity data $F_{observed}$ to geomagnetic anomaly is described in SHIBUYA and TANAKA (1983), only a brief summary is repeated here. $F_{observed}$ is considered to include magnetic intensity of various origins, such as the International Geomagnetic Reference Field F_{IGRF}, diurnal variation by the earth's external field $F_{diurnal}$, magnetic anomalies by the local topographic and geological structures $F_{anomaly}$, and magnetic disturbances by aircraft (flight) condition. F_{IGRF} can be assigned to each acquired total intensity data since the geographic coordinates of each data point are determined as discussed in Section 2. The synthetic calculation of F_{IGRF} is made using the Gauss' coefficients of IGRF 1980 (IAGA WORKING GROUP I-1, 1980) and is reduced to the epoch January 1, 1981. $F_{diurnal}$ can be synthesized from the digitally sampled data of the three-component flux-gate magnetometer at Syowa Station with 2-s intervals. The sensing head was towed by a 20-m coaxial cable and magnetic disturbance by the small aircraft PC-6 is assumed negligible.

Figure 2 illustrates the reduction procedure of each profile. For example, Fig. 2–1 shows from top to bottom (a) observed total intensity data $F_{observed}$, (b) assigned F_{IGRF}, (c) synthetic $F_{diurnal}$, and (d) the reduced $F_{anomaly}$ which is calculated by $F_{observed}-F_{IGRF}-F_{diurnal}$ for Flight M1 profile, respectively. The HF radio communication during the survey flight results in the spike noise on the observed total intensity data and the blank portion corresponds to such noisy portion. It is noted that 10-point moving average (of wave-length ~600 m) is applied to the calculation and illustration of $F_{anomaly}$. Figures 2–2 and 2–3 illustrate similar reduction procedure for Flight M2 and Flight M4 profiles, respectively.

As discussed in HARTMAN *et al.* (1971), the diurnal variation differs from place to place even over a small area of 200 km by 200 km, and no single monitoring station may supply enough information to correct total field data. However, when the time variation becomes long-period, the spatial correlation of magnetic transient becomes high and the long-period drift (longer than 5 min corresponding to a wavelength 20 km) over the region concerned may be represented by the diurnal variation at Syowa Station within the allowance of 20–30 nT uncertainty.

The deduced geomagnetic anomaly profile in Fig. 2 may also have errors through calculation of F_{IGRF} with ill-assigned geographic coordinates. As for Flight M1 and Flight M2, the error in F_{IGRF} is estimated as within 6 nT considering the positioning uncertainty of marker station and the fluctuation of interval speed listed in Table 1. As for Flight M4, try-and-error adjustment of the flight course will aid rough estimate of errors in the obtained geomagnetic anomaly profile.

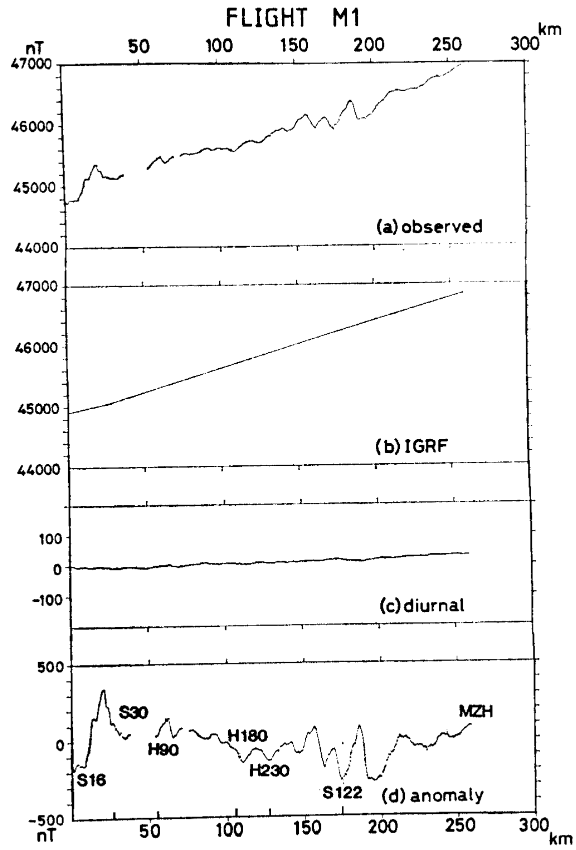

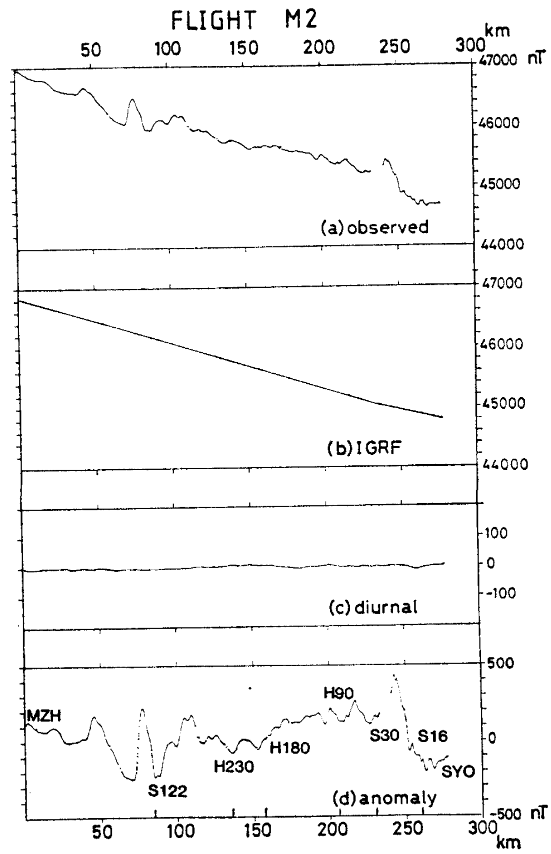

Fig. 2-1. (left) *Fig. 2-2. (right)*

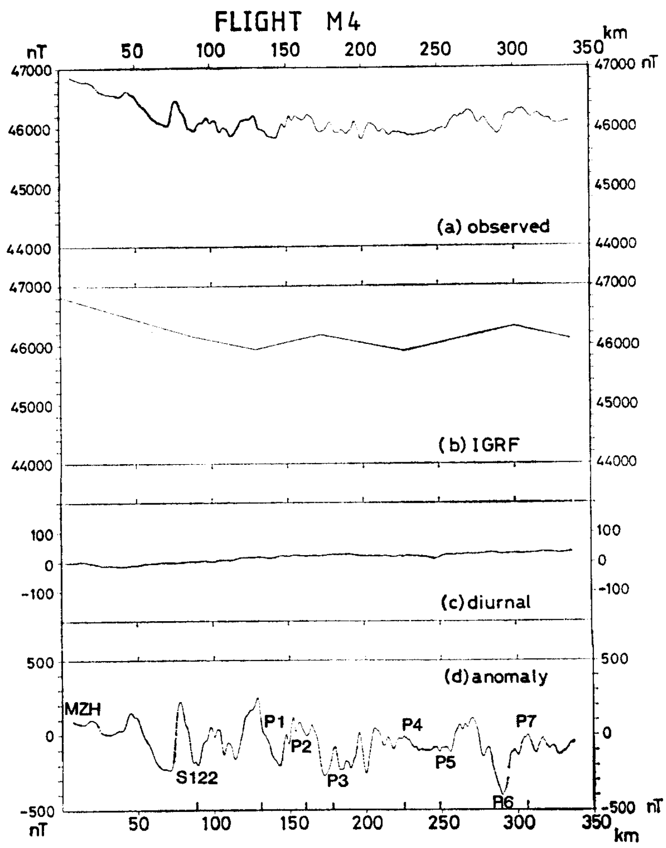

Fig. 2. The reduction of the observed total intensity data to the geomagnetic anomaly. (a) Observed total intensity, (b) synthetic IGRF, (c) diurnal variation at Syowa Station, (d) reduced geomagnetic anomaly. Figures 2-1, 2-2 and 2-3 correspond to Flights M1, M2 and M4, respectively.

Fig. 2-3.

The moraine field is within the katabatic region where the wind speed is rather constant and the wind direction is stable and almost parallel to the slope of the topographic ice sheet. Taking both the possible wind direction (from 225° to 270° measured from geographic north) and the possible wind speed (0 to 20 knots) as parameters, the following nine cases a to i of flight course are considered as illustrated in Fig. 3, where a corresponds to the case with no wind and is identical to the mosaic in Fig. 1. When the wind speed becomes large from 10 to 20 knots, the mosaic is compressed toward the east and is elongated toward the west as exampled in c. The effect on the north-south direction is small as compared with that on the east-west direction. There are several crossing points Q_1, Q_2 and so on in each case of Fig. 3 (*e.g.*, i) and the total intensity data must be identical at these crossing points. The assignment of F_{IGRF} to each $F_{observed}$ becomes different among nine cases with an inconsistence of say 50–100 nT because of different spatial sampling condition. Since the reduced geomagnetic anomaly must be consistent also around these crossing

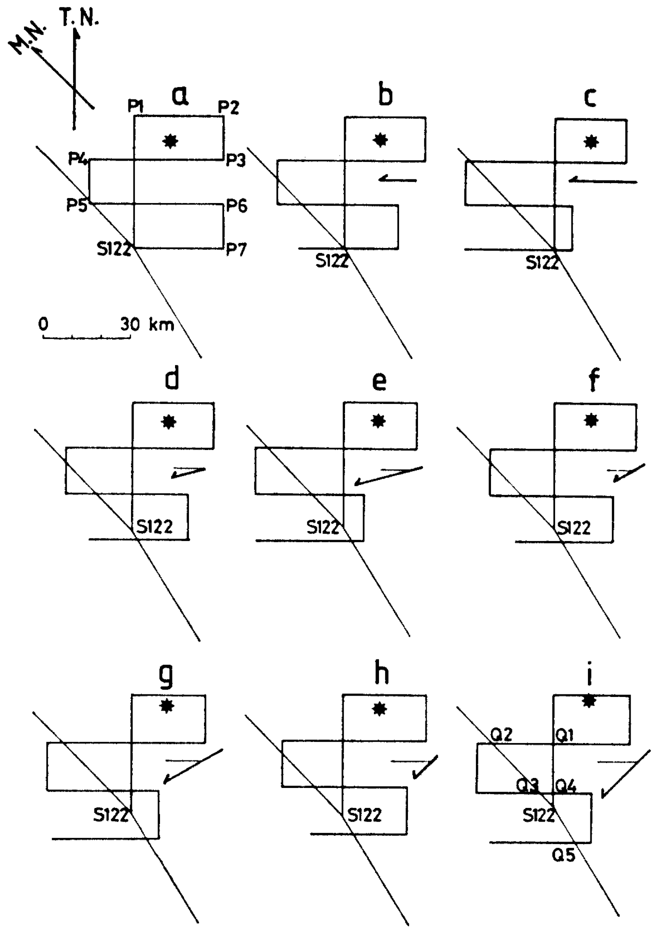

Fig. 3. Effect of wind speed and wind direction on the presumed flight course. Shorter arrow and longer arrow indicate 10-knot and 20-knot wind speed, respectively. The wind direction is assumed from 225° to 270° at intervals of every 15°. T.N. and M.N. indicate true north and magnetic north, respectively. The star indicates moraine field.

points, the most probable case g with the wind speed of 20 knots and the wind direction of 240° can be chosen among the nine cases. These values are not much different from the data of 18 knots and 246° wind direction observed at Mizuho Station by the balloon measurement. Figure 2–3 illustrates thus obtained most probable anomaly over the Flight M4 profile. Taking both the uncertainty from uncorrected diurnal variation and that from ill-assigned F_{IGRF} to each $F_{observed}$, the error in the reduced geomagnetic anomaly is considered to be up to 30–50 nT.

4. Results and Discussions

Figure 4a shows the superposition of the obtained geomagnetic anomaly profile of Flight M2 (broken curve) onto the free-air gravity anomaly profile (solid curve) by KAMINUMA and NAGAO (1984) along Routes S–H–Z. Mizuho Station–S122 portion of Flight M4 geomagnetic anomaly profile almost overlaps that of Flight M2 within 10–20 nT offset. In 1976, the oversnow traverse party of JARE-17 made the ground survey of total intensity data at selected stations along Routes S–H–Z. From the data in Table 2 of NIKI *et al.* (1981), SHIBUYA *et al.* (1984) calculated the synthetic geomagnetic anomaly values at these stations. They are illustrated by solid circles in Fig. 4a and re-tabulated in Table 2. Though the obtained ground data may have an uncertainty of 30 nT, they are consistent with the general trend of aeromagnetically obtained anomaly profile along Routes S–H–Z.

There is 4 hours' lapse time between Flight M1 and Flight M2, and the corresponding DC offset in the diurnal variation is about +30 nT. Even if the above offset is corrected, Flight M1 anomaly profile gives 100–150 nT systematically smaller value as compared with other profiles. Though the reason for this systematic offset is not entirely known yet, it is possible that the off-tuned time gate of precession counting to a slightly shorter repetition cycle rate may give systematically smaller total intensity data. The discrepancy between the obtained ground anomaly data and the anomaly value on the Flight M1 profile at the station in Table 2 becomes larger than the case of Flight M2, and so the Flight M1 anomaly profile is not drawn on Figure 4a as considered possibly due to an erroneous observation.

Thick solid curves in Fig. 4b show the inferred geomagnetic anomaly contours over the surveyed area obtained after the try-and-error adjustment described in the previous section. The thin solid curves in the same figure give the free-air gravity anomaly contours by ABE *et al.* (1978). From the restriction of the reduction uncertainty, the obtained geomagnetic anomalies may have an relative error of 30–50 nT. Therefore, the contouring is made at 100 nT intervals. The data density is still sparse as compared with a rapid change of the geomagnetic anomalies in the region concerned, and the eyes near P1 and around Z30 may be fictitious. Detailed and accurate contouring awaits further survey flights.

Though the contouring of geomagnetic anomalies and free-air gravity anomalies is still in a reconnaissance stage, some characteristic features of the geological structure of bedrock can be deduced. As seen from Fig. 4a, there is a significant geomagnetic anomaly high with an amplitude of 600 nT from Syowa Station to S30. This may correspond to the southwestern edge of the extension of the strong positive anomaly area

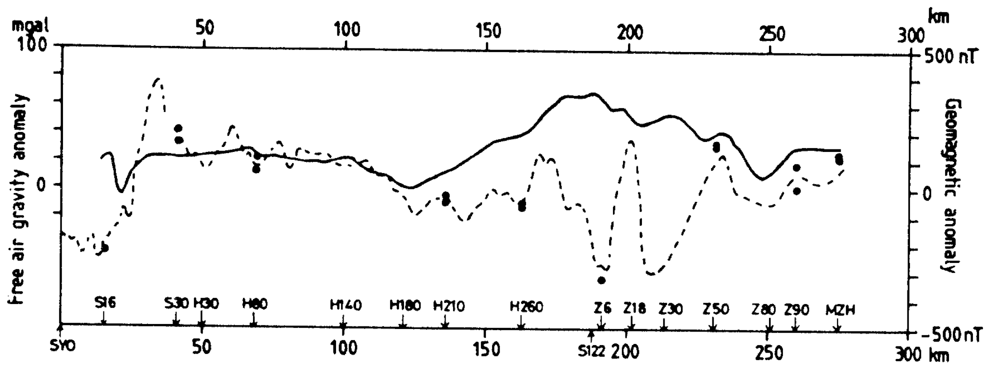

Fig. 4a. Geomagnetic anomaly (broken curve) and free-air gravity anomaly (solid curve) profiles along Routes S–H–Z. Solid circles indicate synthetic geomagnetic anomaly according to Table 2.

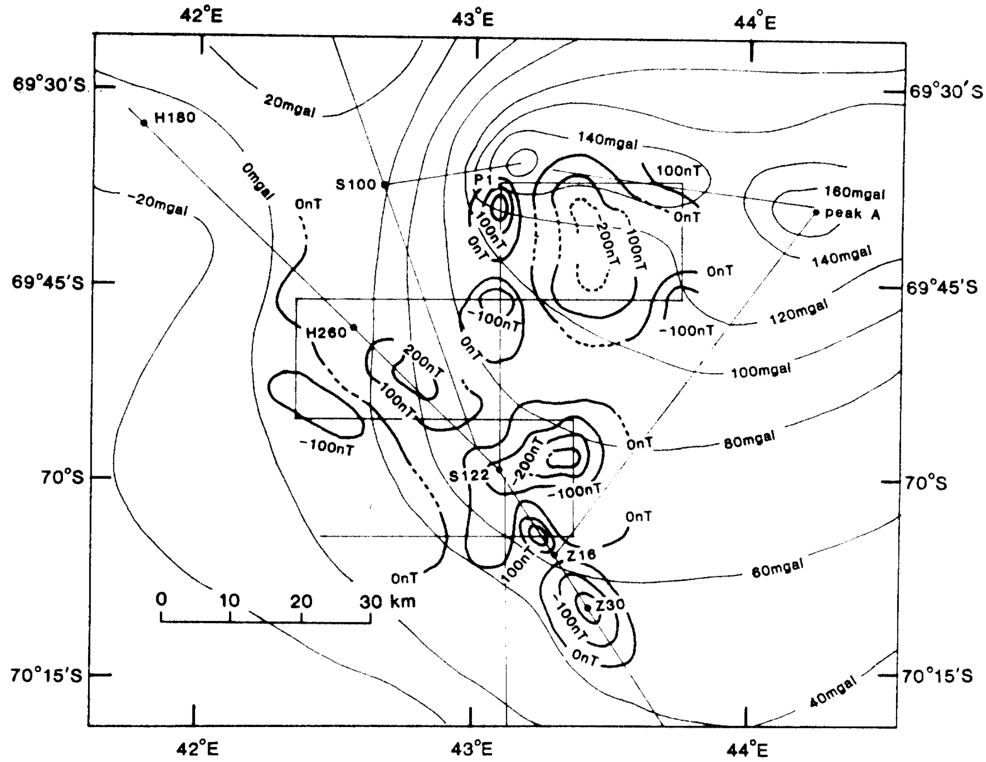

Fig. 4b. Geomagnetic anomaly contours (thick solid curves) and free-air gravity anomaly contours (thin solid curves) over the area concerned. For details, see text.

in Enderby Land revealed by the MAGSAT analysis (Ritzwoller and Bentley, 1983). There is no characteristic free-air gravity anomaly which is associated with the above geomagnetic anomaly. There are other remarkable geomagnetic anomalies around S122 with two adjacent lows and highs with an amplitude of 500 nT ranging from −300 to 200 nT. The amplitude is too large to be adequately explained by the 1000–2000 m subglacial topographic change of the bedrock with the mean susceptibility in the order of 10^{-4}. The wave-length of the above anomalies is short around 10–30 km, which suggests that the source of the geomagnetic anomaly is located at a

Table 2. The ground geomagnetic anomaly values on the traverse route, based on the observed total intensity data by JARE-17 (NIKI et al., 1981) and re-tabulated from SHIBUYA et al. (1984).

Location	Time (45° EMT)	Date	$F_{observed}$ (nT)	F_{IGRF} (nT)	$F_{anomaly}$ (nT)	*K* index at Syowa Station	Latitude	Longitude	Altitude (m)	Ice thickness (m)
S 16	1650LT	15 April	45166	45397	−231	1	69°01.9′S	40°02.9′E	554	
S 30	1445	16 April	45742	45545	197	3	69 03.0	40 42.2	988	1300
	1000	20 August	45666	45508	158	0				
H30	1800	19 August	45662	45579	83	0	69 06.5	40 51.5	1080	
H80	1755	18 April	45869	45755	114	0	69 13.9	41 09.9	1224	1351
	1400	19 August	45782	45720	62	0				
H140	1300	19 April	46093	45995	98	1	69 26.6	41 40.1	1408	1436
	0915	19 August	46036	45959	77	1				
H210	1120	20 April	46261	46281	−20	1	69 42.0	42 16.1	1600	
	1315	18 August	46199	46247	−48	0				
H260	1600	20 April	46439	46487	−48	2	69 52.6	42 43.1	1748	
	0855	18 August	46385	46452	−67	2				
Z6	0950	23 April	46393	46712	−319	2	70 03.9	43 14.5	1962	1494
	1030	17 August	46419	46679	−260	0				
Z50	1810	23 April	47197	47010	187	1	70 22.0	43 46.6	2085	
	1030	16 August	47135	46977	158	1				
Z90	1545	24 April	47318	47228	90	2	70 35.5	44 10.2	2176	1692
	1120	15 August	47196	47196	0	0				
Mizuho Station	1220	10 June	47430	47313	117	0	70 41.9	44 19.9	2230	1998
	1425	12 July	47441	47304	137	0				
	1130	12 August	47420	47295	125	0				

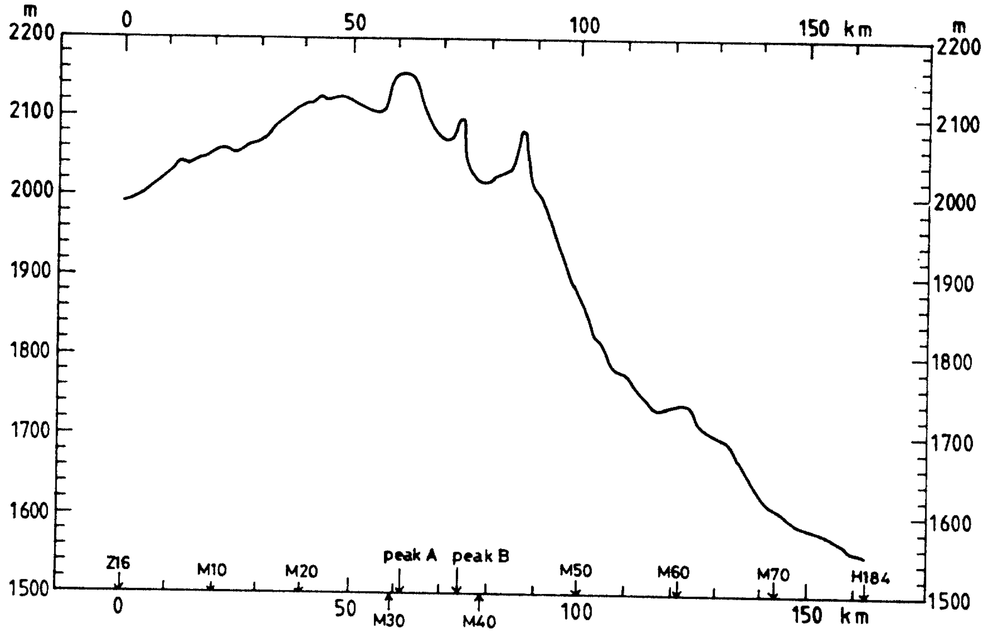

Fig. 5. Surface elevation profile of the ice sheet along Route M. Z16 etc. indicate station names after NARUSE *and* YOKOYAMA *(1975).*

very shallow part of the crust (3–10 km depth) just beneath the 1500–2000 m thick ice sheet.

Figure 5 shows the profile of the ice sheet surface elevation along Route M (Fig. 1) based on the data by NARUSE and YOKOYAMA (1975). The profile has a peak at 2160 m in height and ranges 1500–2200 m with a slope of 5.9×10^{-3} declination westward. The bedrock elevation along Routes S–H–Z is estimated between 0 and 500 m from the radio-echo sounding data (NISHIO *et al.*, 1984) and the mean bedrock elevation of Mizuho Plateau is considered as around 0 m from other geophysical and glaciological observations. On the other hand, the large area of the free-air gravity anomaly high centered at 69°40′S in latitude and 44°10′E in longitude in Fig. 4b, the existence of which is inferred also from the free-air gravity anomaly high from H180 to Z80 in Fig. 4a, is considered as corresponding to a subglacial mound of 2400 m in height from the average bedrock elevation as discussed by SHIBUYA and ITO (1983). Visual observation of many cracks from PC-6 also supports the existence of a steep rise of the bedrock. Then, the moraine field can be considered as having a large mass of bedrock root and the ice thickness beneath the region concerned can be rather thin. The obtained geomagnetic anomalies around S122 and the large area with negative anomaly of −200 nT around 69°40′S and 43°20′E are situated at the peripheral parts of such subglacial mound and more detailed survey flights will elucidate complicated bedrock geological structure beneath the moraine field.

Acknowledgments

The author expresses his sincere thanks to all the members of JARE-21 led by Prof. S. KAWAGUCHI for their kind support during the wintering. Especially T.

MIZUSHIMA, T. YASHIRO and H. OOMORI enabled us to make efficient flight operations by PC-6. Calculations were made with HITAC M180 at the National Institute of Polar Research.

References

ABE, Y., YOSHIMURA, A. and NARUSE, R. (1978): Gravity anomalies and bedrock relief in Mizuho Plateau. Mem. Natl Inst. Polar Res., Spec. Issue, **7**, 37–43.

HARTMAN, R. R., TESKEY, D. J. and FRIEDBERG, J. L. (1971): A system for rapid digital aeromagnetic interpretation. Geophysics, **36**, 891–918.

IAGA WORKING GROUP I-1 (1981): International Geomagnetic Reference Field, 1980, in short articles, notices and useful information. IAGA News, **20**, 100–102.

KAMINUMA, K. and NAGAO, T. (1984): Gravity survey in Lützow-Holm Bay and the Mizuho Plateau, East Antarctica, 1981. JARE Data Rep., **89** (Earth Sci. 1), 59–87.

NARUSE, R. and YOKOYAMA, K. (1975): Position, elevation and ice thickness of stations. JARE Data Rep., **28** (Glaciol.), 7–47.

NIKI, K., YOSHINO, T. and FUKUNISHI, H. (1981): Syowa Kiti fukin no chiziki zenjiryoku bunpu (Contour maps of geomagnetic field intensity in the vicinity of Syowa Station, Antarctica). Nankyoku Shiryô (Antarct. Rec.), **71**, 64–75.

NISHIO, F., ISHIKAWA, M. and OHMAE, H. (1984): Position, elevation and ice thickness of stations between Syowa Station and Mizuho Station. JARE Data Rep., **94** (Glaciol. 10), 6–14.

RITZWOLLER, M. H. and BENTLEY, C. R. (1983): Magnetic anomalies over Antarctica measured from MAGSAT. Antarctic Earth Science, ed. by OLIVER *et al.* Canberra, Aust. Acad. Sci., 504–507.

SHIBUYA, K. (1984): Aeromagnetic survey around Syowa Station, Antarctica. (1) Flights No. 11–M2 by JARE-21. JARE Data Rep., **89** (Earth Sci. 1), 1–58.

SHIBUYA, K. and ITO, K. (1983): On the flow velocity of the ice sheet along the traverse route from Syowa to Mizuho Stations, East Antarctica. Mem. Natl Inst. Polar Res., Spec. Issue, **28**, 260–276.

SHIBUYA, K. and TANAKA, Y. (1983): An aeromagnetic survey over the Shirase Glacier. Mem. Natl Inst. Polar Res., Spec. Issue, **28**, 1–17.

SHIBUYA, K., KAMINUMA, K., IKAMI, A. and ITO, K. (1984): Kôkû jiki sokuryô ni yoru Syowa Kiti to Mizuho Kiti-kan no jiki ijô (Magnetic anomalies along the traverse route from Syowa to Mizuho Stations, East Antarctica). Nankyoku Shiryô (Antarct. Rec.), **83**, 51–61.

SHIMIZU, H. (1978): Outline of studies of the glaciological research program in Mizuho Plateau, East Antarctica, 1969–1975. Mem. Natl Inst. Polar Res., Spec. Issue, **7**, 1–13.

(Received May 2, 1985; Revised manuscript received June 25, 1985)